Holocene Sea-level impacts on Venice Lagoon's coastal wetlands

David Kaniewski, Nick Marriner, Matteo Vacchi, Dario Camuffo, Alexandra Bivolaru, Giovanni Sarti, Duccio Bertoni, Luc Diatta, Nirefs Markakis, Amedeo Martella, et al.

HAL Id: hal-04538817
https://hal.science/hal-04538817

Submitted on 9 Apr 2024

Holocene sea-level impacts on Venice Lagoon's coastal wetlands

David Kaniewski[1]†, Nick Marriner[2]†, Matteo Vacchi[3], Dario Camuffo[4], Alexandra Bivolaru[5], Giovanni Sarti[3], Duccio Bertoni[3], Luc Diatta[6,7], Nirefs Markakis[6], Amedeo Martella[3], Thierry Otto[1], Frédéric Luce[1], Diego Calaon[5], Daniela Cottica[5], Christophe Morhange[6,8]

[1]Centre de Recherche sur la Biodiversité et l'Environnement (CRBE), Université de Toulouse, CNRS, IRD, Toulouse INP, Université Toulouse 3 - Paul Sabatier (UT3), Toulouse, France
[2]CNRS, ThéMA, Université de Franche-Comté, UMR 6049, MSHE Ledoux, 32 rue Mégevand, 25030 Besançon Cedex, France
[3]Dipartimento di Scienze Della Terra, Università di Pisa, Pisa, Italy
[4]Institute of Atmospheric Sciences and Climate, National Research Council of Italy, Corso Stati Uniti 4, 35127 Padua, Italy
[5]Dipartimento di Studi Umanistici, Università Ca' Foscari Venezia, Palazzo Malcanton - Marcorà, Dorsoduro 3484/D, I-30123 Venezia, Italy
[6]Aix Marseille Université, CNRS, IRD, INRA, Collège de France, CEREGE, Aix-en-Provence, France
[7]Aix Marseille Université, CNRS, CCJ, Aix-en-Provence, France
[8]EPHE-Section des Sciences Historiques et Philologiques, AOROC, UMR 8546 - Archéologie et Philologie d'Orient et d'Occident, CNRS/PSL, École normale supérieure, 45 rue d'Ulm, 75230 Paris Cedex 5, France

Corresponding authors: David Kaniewski and Nick Marriner

Email: david.kaniewski@univ-tlse3.fr; nick.marriner@univ-fcomte.fr

Author Contributions: † These authors contributed equally to this work.

Highlights

● New curve for the Holocene RSL history of Venice Lagoon

● Freshwater wetlands transitioned into salt marshes around 6655±70 BP

● A first ecological upheaval resulted from marine intrusions

● Projected sea-level rise will generate a second ecological upheaval

Abstract

Venice Lagoon (Italy), the largest wetland in the Mediterranean basin, is extremely vulnerable to variations in relative sea level (RSL) which is locally defined by an average rising rate of about 2.5 mm per year, resulting from both sea-level change and vertical land movements. The environmental pressures stemming from projected higher RSL rising rates will have a profound impact on Venetian coastal ecosystems with a significant loss of wetlands partly due to a drastic reduction of salt marsh habitats. To understand how changes in marine influence could create such ecological upheaval in the near future, and fully remodel these coastal salt marshes, we reconstructed 5650 years of RSL rise history and land subsidence impacts on ecosystem dynamics during the Holocene transgression of Venice Lagoon. We show that the evolution of ecosystems mainly mirrors the gradual intrusion of salt water that progressively reshaped the coastal vegetation by turning the area into salt lagoon habitats. Before marine influence became dominant, the area was mainly fed by substantial freshwater supplies allowing the development of a diversified alluvial vegetation. Environmental pressures increased markedly about 6800-6600 years ago when seawater began to significantly influence the area, affecting marsh-swamp ecosystems. These marine inputs promoted the spread of halophytic and salt-tolerant vegetation types which laid the foundations for what would become the current salt marsh habitats. Venice Lagoon serves as a stark reminder of how rising sea levels, accompanied by increased saltwater intrusion into freshwater habitats and adjacent lands, can drastically alter and reshape pre-existing ecosystems. The lagoon's long-term ecological record indicates that contemporary fluctuations in RSL pose a substantial ecological threat, potentially culminating in a major upheaval of aquatic habitats in the near future.

1. Introduction

Throughout the 20th and early 21st centuries, relative sea-level (RSL) rise has emerged as a principal driver of coastal transformation (Plater and Kirby, 2011; Williams, 2013), a trend that is projected to intensify throughout this century and beyond due to human-induced global warming (Nicholls and Cazenave, 2010; Woodroffe and Murray-Wallace, 2012; Kulp and

Strauss, 2019). According to the IPCC (2019), global mean sea level, as recorded by tide gauges and satellite altimetry observations, increased from 1.4 mm yr^{-1} over the period 1901-1990 to 3.6 mm yr^{-1} over the period 2006-2015 (Oppenheimer et al., 2019), with a predicted sea-level rise of 0.21 to 0.82 m under Representative Concentration Pathway (RCP) 2.6 and 0.45 to 1.65 m under RCP 8.5 for the year 2100 (Horton et al., 2020). Coastal subsidence may exacerbate sea-level rise, accentuating flooding hazards (Shirzaei et al., 2020), especially in densely populated areas where human-induced subsidence can lead to rates of local RSL much higher than rates of climate-induced RSL (Nicholls et al., 2021; Tay et al., 2022; Wu et al., 2022). RSL rise, resulting from both climate-induced sea-level rise and land subsidence, is a looming threat for many low-lying coastal areas (< 10 m a.s.l.) that already face serious risks due to their high exposure and vulnerability (Magnan et al., 2022). RSL rise is moreover predicted to severely degrade or even damage many coastal ecosystems that will be lost or redistributed (Nicholls and Cazenave 2010; Braun de Torrez et al., 2021). Projections at a global scale suggest that between 20 and 90 % (low and high sea-level rise scenarios) of present-day coastal wetland areas will be lost, resulting in the loss of biodiversity and ecosystem services (Spencer et al., 2016; Schuerch et al., 2018).

The city of Venice (Italy), one of UNESCO's most famous World Heritage Sites, its lagoon and the associated salt marshes are affected by both natural and human-induced land subsidence (Carbognin et al., 2004; Da Lio et al., 2018; Tosi et al., 2018), climate-induced RSL rise (Pirazzoli, 1987; Pirazzoli and Tomassin, 2008; Madricardo and Donnici, 2014; Zanchettin et al., 2021) and human activity in surrounding catchments as well as storm-surge barriers leading to sediment starvation (Nosengo, 2003; Tognin et al., 2021). From the preindustrial era to 1930, land subsidence slightly fluctuated (Wöppelmann et al., 2006) and ranged from 0.6 to 1.6 mm yr^{-1} (Tosi et al., 2013; Zanchettin et al., 2021). Since the 1930s, the subsidence rate has risen, ranging from 1.0±0.7 (period 2003-2010) to 1.7±0.5 mm yr^{-1} (period 2014-2020; Tosi et al., 2013; Zanchettin et al., 2021). For the lagoon, the average subsidence rates for the 21st century are estimated to be 3-4, 1-2 and 2-3 mm yr^{-1} for the northern, central and southern parts, respectively (Tosi et al., 2018; Zanchettin et al., 2021). As the city and lagoon undergo gradual subsidence, The rate of sea level rise (RSL) stands out as a critical factor shaping the future trajectory of the region. The current estimate of the average rate of RSL rise during the period 1872-2019, based on tide-gauge data after removing subsidence effects, is 1.23±0.13 mm yr^{-1} (Zanchettin et al., 2021). Combining the two contributors (RSL and subsidence) an average RSL rising rate of 2.5 mm yr^{-1} is observed for the past 150 years. The predicted RSL rise for

the year 2100, only resulting from natural local subsidence, is about 10 cm relative to the late 20th century. The climate-induced RSL rise lies in the ranges of 21-52 cm (RCP2.6) and 48-100 cm (RCP8.5; Zanchettin et al., 2021).

Venice Lagoon (~550 km^2; mean depth 1.1 m; tidal range 0.6-1 m) is a shallow microtidal basin defined by a complex network of channels and intertidal flats forming a major salt marsh complex (Carniello et al., 2009; Ivajnšič et al., 2018). The extensive intertidal salt marshes are located mainly in the southwest and northeast parts of the lagoon (Day et al., 1998). However, these ecologically valuable and protected habitats are already threatened (~12,000 ha at the beginning of the century, ~4,000 ha in 2018) mainly due to human activities (Carniello et al., 2009; Sarretta et al., 2010; Ivajnšič et al., 2018). Land subsidence and sea-level change will further affect the geography of salt marsh habitats in the near future. Projected losses for 2050 concern all habitats (Bellafiore et al., 2014), especially the halophytic vegetation, key to tidal salt marsh stability and functioning (Ivajnšič et al., 2018). Its loss is likely to exacerbate any projected adverse effects of climate change. Moreover, the loss of salt marsh vegetation would be reflected in the whole biota.

Here, using multiproxy observations from Venice Lagoon (Lio Piccolo, Italy), but with wide implications for similar coastal wetlands worldwide, we reconstructed the effects of rising sea level on coastal ecosystems at a plurisecular scale. We investigate 5650 years of RSL rise and land subsidence impacts on ecosystem dynamics based on the Holocene transgression history of Venice Lagoon. These datasets were used to identify the level of alteration of coastal habitats and the magnitude of impact on ecological systems to infer potential effects of the current RSL trend in the northern Adriatic. Understanding the past is crucial for gauging the extent of ecological transformation and reconfiguration triggered by rising sea levels.

2. Venice Lagoon

Venice Lagoon, situated in the North-Western Adriatic, is bounded by the Sile River to the North and the Brenta River to the South (Taramelli et al., 2021). The area receives freshwater from eleven major tributaries plus several minor rivers and a number of human-regulated channels used primarily for agriculture. The lagoon is connected to the sea by three inlets and is subdivided into three basins, Lido in the North (276 km^2), Malamocco in the middle (112 km^2) and Chioggia in the South (111 km^2). A large part of the lagoon (~80%) consists of mudflats, tidal shallows and salt marshes of high ecological value but today under threat. The

salt marshes are covered by dense populations of halophytic vegetation species such as *Arthrocnemum macrostachyum*, *Aster tripolium*, *Halimione portulacoides*, *Limbarda crithmoides*, *Limonium narbonense*, *Puccinellia festuciformis*, *Salicornia procumbens* ssp. *procumbens*, *Salicornia veneta*, *Sarcocornia fruticosa*, *Spartina maritima,* and *Suaeda maritima*. This vegetation occupies the numerous intertidal flats (Silvestri and Marani, 2004; Ivajnšič et al., 2018; Taramelli et al., 2021). Underwater spermatophytes such as *Cymodocea nodosa*, *Zostera marina*, *Nanozostera noltii*, *Ruppia cirrhosa,* and *Ruppia marítima* have colonized the lagoon (Sfriso et al., 2009). Marginal freshwater habitats are dominated by *Phragmites australis* and *Juncus maritimus*. Coastal areas are mainly dominated by patches of *Pinus pinea*.

3. Materials and methods

3.1. RSL in Venice

We reconstructed the Holocene sea-level history of Venice Lagoon (Fig. 1) by combining new Sea-Level Index Points (SLIPs, i.e., a point that constrains the palaeo sea-level in space and time; Shennan et al., 2015) from our study with data points from Vacchi et al. (2016; Fig. 2a). A total of 53 SLIPs was assembled from radiocarbon-dated samples retrieved from sediment cores collected across the lagoon. All radiocarbon ages were re-calibrated into sidereal years with a 2σ uncertainty using the most recent Calib-Rev 8.2 calibration curve. The IntCal20 dataset was used for terrestrial samples and the Marine20 dataset for marine samples (Reimer et al., 2020). A local marine reservoir correction (ΔR) of 306 ± 80 ^{14}C yr was applied for marine shells, recalculated with the Marine20 dataset (Heaton et al., 2020). The indicative range (i.e., the relationship of each sample to the former MSL) of each RSL index point was determined according to Vacchi et al. (2016, 2021) and the standardized methodology for the reporting of RSL data developed by HOLSEA (Khan et al., 2019). We employed the Errors-In-Variables Integrated Gaussian Process (EIV-IGP) model (Cahill et al., 2016) to derive rates of RSL change from SLIPs (Fig. 2b), with a local GIA correction of -0.187 mm^{-1} (Marriner et al., 2023). The EIV-IGP model utilizes a Gaussian Process prior on RSL rate estimates and integrates this rate process to obtain estimations of the underlying RSL process (Cahill et al., 2016). To address temporal uncertainty, this inverse approach is embedded within an Errors-In-Variables framework. The RSL uncertainties related to the SLIPs are incorporated into the statistical model by introducing observation-specific error terms in the RSL data model. Overall, this

modeling approach provides a comprehensive quantification of uncertainty in both RSL estimates (Fig. 2b) and the estimated rates of RSL change over time (Fig. S2 and Fig. S3a-c; Cahill et al., 2016). We also performed an EIV-IGP model run which included RSL data from Camuffo et al. (2017) and Camuffo (2022; Fig. S4a-b). To determine the rate of subsidence during the Holocene, we subtracted the altitude of 53 SLIPs from the ICE6G glacial isostatic adjustment (GIA) model (Fig. S3a). We then divided the residuals by time (to 0 BP) to obtain average subsidence rates in millimeters per year (mm^{-1}).

3.2. Core and chronology

The core LPC21 C02 was drilled in the salt marshes of Lio Piccolo, Cavallino-Treporti (45°29'35.49"N, 12°28'58.72"E, 2 m a.s.l.), Venice Lagoon (Fig. 1). The lithology of the core LPC21 C02 is heterogeneous with a mostly clay matrix mixed with silts and scarce sand particles (Fig. S1). The upper layer (3 m) was not studied due to anthropogenic disturbance. Sampling was done according to the different depositional layers. On average, this corresponds to one sample every 5.5 cm (average 5.5±2.5 cm), but with some variations to respect the core stratigraphy. The chronology of the core LPC21 C02 (Fig. S1) is based on seventeen ^{14}C dates performed on short-lived terrestrial samples (small leaves and seeds). The absence of botanical macro-remains between 950 and 650 cm depth prevented an accurate dating of this part of the sedimentary sequence. All the botanical macro-remains were sent to Beta Analytic (Florida). The ^{14}C dates were calibrated to 2σ using Calib Rev 8.0.1 (IntCal20). All the calibrated ages are denoted in BP. The associated dating error (2σ) is averaged to ± 70 years for the whole sequence. The core LPC21 C02 covers the period 8255±70 - 2375±70 BP.

3.3. Palaeoecological data

A total of 198 samples from the core LPC21 C02 were prepared for pollen analysis using standard procedures for clay-silt samples (Faegri and Iversen, 1989). Pollen grains were counted under x400 and x1000 magnification using an Olympus microscope. The mean pollen sum is 451±68 pollen grains, with a minimum of 331. The median value is 436 pollen grains, with a 25th percentile of 408 and a 75th percentile of 480 pollen grains. The mean number of taxa is 64±5 with a minimum of 42. Pollen frequencies (expressed as percentages) are based on the terrestrial pollen sum, excluding local marsh plants (macrophytes and helophytes) and

spores of non-vascular cryptogams. Marsh plant frequencies (wetland component group) were calculated by adding the local macrophytes and helophytes to the terrestrial pollen sum. Dinoflagellate cysts (marine plankton) were counted on pollen slides and are reported as concentrations (cysts per cm^{-3}). Foraminifers, ostracods, marine bivalves and *Charophyta* debris were extracted from the same samples as the pollen grains and dinoflagellate cysts to avoid any analytical bias. The marine (foraminifers, ostracods, marine bivalves) and freshwater (*Charophyta*) debris were picked from the washed sediment fraction and are displayed as concentrations (scores: remains per 10 cm^{-3}).

3.4. Marine components

The marine component signal is based on an average incorporating foraminifers, ostracods, marine bivalves and dinoflagellate cysts. The concentrations were transformed into z-scores and the resulting data were averaged (with a standard deviation). As we focused on trends, a regular 20-yr chronological interpolation and a 400-yr moving average were applied to the dataset. The scores were then plotted on a linear age-scale with the 2σ dating error and the standard deviation (Fig. 2c). The long-term trend was calculated using polynomial models (termed PM; $P_{value} < 10^{-3}$) with a P_{value} based on a F test - two-tailed, with no adjustment.

3.5. Ecosystem dynamics

The pollen dataset (frequencies) was first analyzed using a cluster analysis (descending type; Fig. S5) to calculate a dendrogram, using branches as ecological distances between groups of taxa. The test was performed using *Paired group* as the algorithm and *Correlation* as the similarity measure. Each cluster was summed to generate pollen-derived vegetation patterns (PdVs; Fig. S6) and assigned to a potential location, from the alluvial floodplain to the salt marshes, referring to modern patches of vegetation. A regular 20-yr chronological interpolation was applied to the dataset (Fig. S6). The long-term trend of each PdV was calculated using a 400-yr moving average and a polynomial model (termed PM; $P_{value} < 10^{-3}$; Fig. S6) with a P_{value} based on a F test - two-tailed, with no adjustment. The average value of each PdV is underlined.

The PdVs were transformed into z-scores and a second cluster analysis (descending type; Fig. 3a) was calculated (with *Paired group* as algorithm and *Correlation* as the similarity measure) to test the ordination of terrestrial vegetation against charophytes and marine indicators. A

Spindle diagram was then performed based on z-scores and contrasted with the RSL estimate (Fig. 3b).

The ecosystem dynamics signal is based on a principal component analysis (PCA) which was subsequently performed to test the ordination of samples by assessing major changes in the PdV-scores (frequencies; Fig. 4a). The first axis (PCA-Axis 1), which carries the maximum variance (88.9% of total variance), was extracted and termed *coastal vegetation*. The PdVs resulting from an alluvial influence are loaded by the positive PCA-Axis 1 scores while the PdVs showing a marine influence are loaded by the negative scores (Fig. S5). A $\pm$ 1σ error was added to the PCA-Axis 1 scores based on the 2.5-97.5[th] percentiles. A regular chronological interpolation (20-yr) was applied to the PCA-Axis 1 scores. The long-term trend was calculated using a 400-yr moving average and a polynomial model (termed PM; $P_{value} < 10^{-3}$; Fig. 4a) with a P_{value} based on a F test - two-tailed, with no adjustment.

3.6. Environmental evolution

The marine components and the coastal vegetation proxy were further contrasted with the RSL estimate using long-term trends (Fig. 4b). The 400-yr moving average and the polynomial models (termed PM; $P_{value} < 10^{-3}$; Fig. 4a) were used to highlight the link between RSL rise, increases in marine components and changes in coastal vegetation. Each PdV influenced by the alluvial system was also plotted against RSL rise using long-term trends (Fig. S7). An average and a standard deviation were calculated using all the taxa included in each PdV.

The link between coastal vegetation and the RSL estimate was tested, ranking the RSL values in ascending order and retaining the associated coastal vegetation scores (Fig. S8a). Because we focused on trends, coastal vegetation and RSL estimates were smoothed using a polynomial model (termed PM; $P_{value} < 10^{-3}$; Fig. S8a) with a P_{value} based on an F test - two-tailed, with no adjustment. The results are shown with the $\pm$ 1σ error. The same process was applied for the link between the marine components and the RSL estimate (Fig. S8a). Cross-correlations were also performed to ascertain the best temporal match between i) the RSL estimate *versus* coastal vegetation, and ii) marine components *versus* coastal vegetation. The correlation coefficient (R^2) is provided, with a focus on the Lag_0 value (with the associated P_{value}), and the significant thresholds are set at +0.50 and -0.50.

We finally produced a ratio based on the two main PdVs (halophytes and salt-tolerant plants/mixed oak forest - with a 95% two-tailed confidence interval), using the polynomial model (termed PM; $P_{value} < 10^{-3}$) to decipher if RSL rise and increasing ratio scores followed the same trend during the last 8000 years (Fig. S8b).

3.7. Data availability

The data supporting our results are provided as Supplementary data to this article.

4. Results

4.1. RSL estimate

A total of 53 SLIPs was used to frame the Holocene sea-level evolution of Venice Lagoon (Fig. 2a). At 8010±135 BP, the SLIPs-derived model (SLIPs^{dm}) places the RSL at 11.7±1.8 m below current MSL (^{bc}MSL) with a rising rate of 1.4±4.6 mm yr^{-1} (Fig. S2). The SLIPs^{dm} suggests that RSL rose rapidly from 6990±135 (-9.3±0.6 m ^{bc}MSL - rising rate of 3.9±2.3 mm yr^{-1}) to 5990±135 BP (4.4±1.6 m ^{bc}MSL - rising rate of 3.7±2.3 mm yr^{-1}). This was followed by a slowdown which is consistent with the progressive reduction in glacial meltwater inputs (Milne et al., 2005; Roy and Peltier, 2018). From 5590±135 to 3190±135 BP, the SLIPs^{dm} delineates a significant reduction in the rising rates (average 0.18±1.05 mm yr^{-1}) and an oscillating system essentially controlled by land subsidence (> 1 mm yr^{-1} with a maximum score of 1.16±0.23 mm yr^{-1}; Fig. S3a-c) and sedimentary compaction. This process remained active until 2490±135 BP when the RSL stabilized around 1.5±0.7 ^{bc}MSL, reaching the highest score (0.8±0.6 ^{bc}MSL) at 1490±135 BP (Fig. 2b). Moreover, the most recent part of the RSL estimate (Fig. S4a-b) falls within the scores of previous Venice sea-level reconstructions (Camuffo et al., 2017; Camuffo, 2022). When the whole dataset is considered, the average rising rate can be estimated to be 1.4±0.3 mm yr^{-1} (using the standard error). Focusing on the last 6000 years, the average rising rate can be estimated to be 0.6±0.2 mm yr^{-1} (using the standard error).

4.2. Evolution of marine components

The core LPC21 C02 included many debris/fragments of foraminifers, ostracods and marine bivalves as well as numerous dinoflagellate cysts. These biological indicators, markers of an

increasing marine influence in the sedimentary deposits, rose significantly in the sequence after 7035±70 BP when the marine transgression progressively flooded the upper Adriatic coastal plain (Fig. 2c). A first high score (0.61±0.2) was reached at 5875±70 BP considering the 400-yr long-term trend (Fig. 2c). The marine component proxy evolved in a manner similar to the RSL oscillations, with a slight decreasing trend from 5255±70 to 4595±70 BP centered on a relative drop (0.25±0.2) at 4935±70 BP. The signal finally stabilized at relatively high scores from 4075±70 BP (average 0.99±0.11 from 4075±70 to 2375±70 BP). The growing influence of seawater in the zone that became Venice Lagoon, attested by both RSL rise and marine components, changed the local conditions with strong and recurrent inputs of salt into the ancient freshwater-fed area.

4.3. From wetlands to salt marshes

Before the marine transgression reached Venice, the PdVs (Fig. S5) suggest that the area was mainly a freshwater basin as attested by both charophytes, macrophytes (up to 10.7%), helophytes (up to 14.1%), fen trees (up to 25.2%) and a wet meadow (up to 17.8%; Fig. 3a and Fig. S6). The upper zones were likely colonized by a mixed oak forest with intrusions of mountain components. Pollen deriving from these upper zones were probably carried into the basin by freshwater inputs from major tributaries as well as minor waterways (Fig. 3b and Fig. S6; Bondesan, 2017). A first significant change in ecosystem dynamics occurred from 7795±70 to 7515±70 BP suggesting either an early influx of salt water into the area or a decrease in freshwater inflow, which could explain the drop in pollen from the upper zones, and the development of a pine woodland. While the gradual rise of salt marsh vegetation (halophytes and salt-tolerant plants) has occurred since 7555±70 BP, the first significant (above average) increase with recurrent values above this threshold was recorded from 6815±70 to 6265±70 BP (Fig. S6). This increase constitutes the first stage of marsh colonization by the halophytes as suggested by a plateau phase where the scores change very little (average of 40.1±5.3%). However, since 6175±70 BP, the marine transgression completely remodeled the habitat, creating a major ecological upheaval (Fig. 3b), reducing all alluvial PdVs (all below average) and generating a large increase in salt marsh plants (59.8% at 5955±70 BP). The extent of the salt marshes seems, however, to have oscillated from 5575±70 to 4315±70 BP as suggested by variations in halophytes (average 42.4±3.9%). This resulted in the development of a pine woodland and a slight increase in alluvial PdVs (Fig. S6). According to the ecosystem

dynamics, the salt marshes became heavily dominant around 4215±70 - 4075±70 BP in Venice Lagoon (Fig. 3b).

4.4. Ecological upheaval

The PCA-Axis 1, loading 88.9% of the total variance, clearly depicts the ecological upheaval that occurred between 7000 and 6000 BP (Fig. 4a). The threshold (0 score) was exceeded at 6655±70 BP, indicating that the halophytes became the main ecosystem component in the salt-water habitats under development. When sea-level change and evolution of marine components are compared and contrasted with the PCA-Axis1, using long-term trends, the widespread impact of sea water on the coastal dynamics seems a decisive factor (Fig. 4b). This argument is strengthened by the cross-correlations sea-level change *versus* PCA-Axis 1 (Lag$_0$ -0.93; P$_{value}$ < 0.001) and marine components *versus* PCA-Axis 1 (Lag$_0$ -0.95; P$_{value}$ < 0.001) which both strongly suggest that marine transgression of northern the Adriatic coast was the main forcing agent behind observed changes in ecosystem dynamics (Fig. S7). Using sea-level change as the driver, the marine components and coastal vegetation dynamics both align with this environmental constraint (Fig. S8a). Moreover, when the salt marsh plants are contrasted with the mixed oak forest, using a ratio, the signal is coherent with the RSL rise (Fig. S8b). All the proxies depict an ecological upheaval led by sea-level change as a major constraint.

5. Discussion

This study, based on a new curve for the Holocene RSL history of the Venice Lagoon, has provided an assessment of when and how freshwater wetlands transformed into salt marshes. Our data show that these marine intrusions created a first major ecological upheaval in the lagoon 6655±70 years ago. Our study also provides insights into how projected RSL rise will generate a second major ecological upheaval in the near future.

5.1. Effect of sea water

Before the marine seawater reached the northern Adriatic coasts, the area near Venice was already a wetland, fed by freshwater tributaries and outflowing groundwater as suggested by the high concentrations of macrophytes and helophytes (Bondesan, 2017). Comparable

arguments were proposed in an environmental study centered on the coastal plains stretching from the Sile River to the Tagliamento River (Miola et al., 2010). The proposed date of 6815±70 BP at Lio Piccolo for the first stage of significant marsh colonization by the halophytes strengthens the ~ 6700 BP date previously suggested for sites located further inland (Miola et al., 2010). The PdV mixed oak forest and mountain components identified during this early stage is consistent with the vegetation found in cores drilled in the urban area of Venice (ARS-S1; Serandrei-Barbero et al., 2005; Donnici et al., 2012) and in the eastern part of the lagoon (BH2; Canali et al., 2007). The biological indicators of this PdV in core LPC21 C02 likely originate from areas outside the marsh where probably thicker and more evolved soils are found and were transported towards Lio Piccolo by recurrent freshwater inputs. The plant community of the ancient flooded area was most likely composed of macrophytes, helophytes, fen trees and wet meadows, forming a freshwater wetland of great ecological diversity. Such landscapes can be found nowadays in the coastal wetland north of Ravenna (the Bardello; Piccoli and Merloni, 1989). Seawater intrusions affected this initial wetland by causing major physical changes in water and soils (salinity, pH, sediment and nutrient fluxes; Bonometto et al., 2019), even on the mainland where the salt probably reached the coastal water tables (Di Sipio et al., 2006). The water probably became increasingly saline due to growing evaporation (leading to high salt concentrations in groundwater), strong evapotranspiration, evaporation and transpiration of sea water by halophytes in the newly formed salt marshes, salt secretion by plants, and the leaching of salts deposited at the surface (e.g. Bonometto et al., 2019). This created an ecological upheaval that completely redefined the habitats in the forming lagoon.

5.2. The salt marshes

According to the ecological parameters recorded at Lio Piccolo, Venice Lagoon gradually transitioned into a salt zone from 7000 BP onwards but became a permanent salt marsh area after 5000 BP. It has been previously suggested, based on foraminifera, that ancient salt marshes in the lagoon (since ~ 4350±196 BP) were close to the current one (Barbero et al., 2004). This argument is supported by the halophytic vegetation assemblage from the core LPC21 C02, which includes families or genus that have modern analogues such as Amaranthaceae (e.g. *Arthrocnemum macrostachyum*, *Salicornia procumbens* ssp. *Procumbens*, *Salicornia veneta*, *Sarcocornia fruticosa*), Apiaceae (e.g. *Crithmum maritimum*), Asteraceae (e.g. *Aster tripolium*, *Dittrichia crithmoides, Limbarda crithmoides*), Chenopodiaceae (e.g. *Atriplex portulacoides*, *Suaeda maritima*), Plumbaginaceae (e.g. *Limonium narbonense*) and Poaceae (e.g. *Catapodium*

marinum, Puccinellia festuciformis; *Spartina maritima*; Silvestri and Marani, 2004; Miola et al., 2006, 2010; Ivajnšič et al., 2018; Taramelli et al., 2021). Other plants such as *Artemisia*, *Ephedra fragilis*, *Matthiola*, *Medicago*, *Polygonum* or families such as Brassicaceae (e.g. *Cakile maritima*), Caryophyllaceae (e.g. *Spergularia marina*), Euphorbiaceae (e.g. *Euphorbia* sp.), Fabaceae or Liliaceae are usually found on coastal Adriatic shores (Wolff, 1968; Stancic et al., 2008; Milović et al., 2016). Such mixed assemblages of salt-tolerant taxa have also been identified in coastal Istria (Croatia - northern Adriatic; Kaniewski et al., 2018, 2021). In Venice Lagoon, it is evident that RSL changes, initially instrumental in establishing a favorable physical environment for halophytes, will soon exert an influence on the salt marsh ecosystems. These ecosystems, having thrived and adapted locally for ~6800-6600 years under the influence of the marine environment, stand ready to face the imminent impacts of external changes in the near future. This biological heritage, established thanks to marine contributions and representative of Venice Lagoon, is nowadays under threat (degradation or even complete disappearance) by RSL rise.

5.3. Forecasted impacts of RSL rise

Present-day and future sea-level changes accentuated by land subsidence (Madricardo and Donnici, 2014; Tosi et al., 2018; Zanchettin et al., 2021) and increased erosion resulting from deeper tidal flats (Carniello et al., 2009) will potentially create a second ecological upheaval in Venice Lagoon. While it has been shown that salt marshes can be resilient to RSL rise (Rizzetto and Tosi, 2011), the ecosystems that populate these habitats may, conversely, be profoundly affected (Carniello et al., 2009; Sarretta et al., 2010). It has been suggested that by 2075, 37 to 51% (model-based scenarios or linear scenario respectively) of Venice Lagoon's coastal habitats could lie under water (Ivajnšič et al., 2018). Although nearly all habitats will manifest a decrease in their extent by 2050 and beyond, the different types of marshes will respond differently to RSL rise, with clear disparities between the northern and southern parts of the lagoon (Ivajnšič et al., 2018). While coastal erosion could begin and develop intensively in the northern lagoon before expanding to the southern part in the second half of the century (Ivajnšič et al., 2018), a study covering the period 1901-2003 highlights a slower erosive trend in the northern part compared to the faster erosion in the central and southern parts (Carniello et al., 2009). The LPC21 C02 core shows indirectly, through vegetation dynamics, the gradual transformation of the northern part of the lagoon. It also shows how saline seawater intrusions created a first major ecological upheaval during the Holocene, impacting or even eradicating

the freshwater habitats that characterized the area. Future physical changes due to RSL rise will likely exceed those that have occurred over the past 6800-6600 years (taking the first marine imprint in the area), affecting current habitats through shrinkage, submergence and erosion. Venice Lagoon will probably, like 7000-6000 years ago, change profoundly, creating a new environment which will be shaped by RSL rise, land subsidence, climate pressures, urbanization and anthroposcapes, all due to human behavior.

5.4. Other contributory factors

Salt marshes and coastal dynamics have been and will be influenced by other contributing factors. Human activity within upstream catchments has led to sediment starvation affecting vertical accretion and vegetation colonization (Gambolati et al., 1998; Mel et al., 2022), resulting in the drowning of salt marshes and a reduction in their aerial extent (Tognin et al., 2021). Storm surges still pose severe problems for Venice and its lagoon (Lionello et al., 2012), damaging urban heritage (Carbognin et al., 2010; Mel and Lionello, 2014) and impacting the coastal area as well as salt marshes by causing severe flooding (Troccoli et al., 2012). While threatening, storm surges also act as a powerful agent of salt-marsh sedimentation due to sediment reworking. This process will probably be lowered by storm-surge barriers, temporarily closing the lagoon inlets, affecting the redistribution of reworked sediment within the lagoon and leading to sediment deprivation (Nosengo, 2003; Tognin et al., 2021). Moreover, numerous erosive processes affect the coast (Adriano et al., 2005; Angeli et al., 2005; Amos et al., 2010) such as wind-wave power (Tommasini et al., 2019) and human activities such as intensive clam fishing or tourism (Sarretta et al., 2010). All of these processes will affect, along with RSL rise, the salt-marsh habitats.

6. Conclusions

Venice Lagoon is a legacy of the Holocene marine transgression and has already been affected by human-induced sea-level rise, which are significantly reshaping the northern area of the Adriatic and its coastal ecosystems. Throughout the Holocene, the lagoon experienced influences solely from natural forces. In contrast, the Anthropocene era is characterized by a reversal, as unprecedented and substantial pressures, originating from human activities such as RSL rise, land subsidence, erosion and alterations in land use, have come to the forefront. The

combined effect of each threat will have the greatest impact on salt marsh habitats. Our study implies that the preservation of these lagoon habitats is jeopardized not by a single factor but by a complex interplay of interacting variables. This dynamic interaction is anticipated to shape a new model for the lagoon, reflecting the ongoing and future threats it faces.

References

Adriano, S., Chiara, F., Antonio, M., 2005. Sedimentation rates and erosion processes in the lagoon of Venice. Environ. Int. 31, 983-992.

Amos, C. L., Umgiesser, G., Ferrarin, C., Thompson, C. E. L., Whitehouse, R. J. S., Sutherland, T. F., Bergamasco, A., 2010. The erosion rates of cohesive sediments in Venice lagoon, Italy. Cont. Shelf Res. 30, 859-870.

Angeli, M. G., Gasparetto, P., Marabini, F., Menotti, R., Merzanis, A., Pontoni, F., 2005. The evolution of the Adriatic coastal zone (Italy) between the Gabicce promontory and the Tronto River mouth. WIT Trans. 78, DOI: 10.2495/CE050161.

Barbero, R. S., Albani, A. D., Bonardi, M., 2004. Ancient and modern salt marshes in the Lagoon of Venice. Palaeogeogr. Palaeoclimatol. Palaeoecol. 202, 229-244.

Bellafiore, D., Ghezzo, M., Tagliapietra, D., Umgiesse, G., 2014. Climate change and artificial barriers effects on the Venice laggon: Inundation dynamics of salt marshes and implications for halophytes distribution. Ocean Coast. Manag. 100, 101-115.

Bondesan, A., 2017. Geomorphological processes and landscape evolution of the Lagoon of Venice, in: Soldati, M., Marchetti, M. (Eds), Landscapes and landforms of Italy - World geomorphological landscapes, Springer, Cham., pp. 181-191.

Bonometto, A., Feola, A., Rampazzo, F., Gion, C., Berto, D., Ponis, E., Boscolo Brusà, R., 2019. Factors controlling sediment and nutrient fluxes in a small microtidal salt marsh within the Venice Lagoon. Sci. Total Environ. 650, 1832-1845.

Braun de Torrez, E. C., Frock, C. F., Boone IV, W. W., Sovie, A. R., McCleery, R. A., 2021. Seasick: why value ecosystems severely threatened by sea-level rise? Estuaries Coast 44, 899-910.

Cahill, N., Kemp, A. C., Horton, B. P., Parnell, A. C., 2016. A Bayesian hierarchical model for reconstructing relative sea level: from raw data to rates of change. Clim. Past 12, 525-542.

Camuffo, D., 2022. A discussion on sea level rise, rate ad acceleration. Venice as a case study. Environ. Earth Sci. 81, 349. https://doi.org/10.1007/s12665-022-10482-x

Camuffo, D., Bertolin, C., Schenal, P., 2017. A novel proxy and the sea level rise in Venice, Italy, from 1350 to 2014. Clim. Change 143, 73-86.

Canali, G., Capraro, L., Donnici, S., Rizzetto, F., Serandrei-Barbero, R., Tosi, L., 2007. Vegetational and environmental changes in the eastern Venetian coastal plain (Northern Italy) over the past 80,000 years. Palaeogeogr. Palaeoclimatol. Palaeoecol. 253, 300-316.

Carbognin, L., Teatini, P., Tosi, L., 2004. Eustacy and land subsidence in the Venice Lagoon at the beginning of the new millennium. J. Mar. Syst. 51, 345-353.

Carbognin, L., Teatini, P. Tomasin, A., Tosi, L., 2010. Global change and relative sea level rise at Venice: what impact in term of flooding. Clim. Dyn. 35, 1039-1047.

Carniello, L., Defina, A., D'Alpaos, L., 2009. Morphological evolution of the Venice lagoon: Evidence from the past and trend for the future. J. Geophys. Res. 114, F04002. http://dx.doi.org/10.1029/2008JF001157.

Da Lio, C., Teatini, P., Strozzi, T., Tosi, L., 2018. Understanding land subsidence in salt marshes of the Venice Lagoon from SAR Interferometry and ground-based investigations. Remote Sens. Environ. 205, 56-70.

Day, J. W. Jr., Rismondo, A., Scarton, F., Are, A., Cecconi, G., 1998. Relative sea level rise and Venice lagoon wetlands. J. Coast. Conserv. 4, 27-34.

Di Sipio, E., Galgaro, A., Rapaglia, J., Zuppi, G. M., 2006. Salt water contamination on Venice Lagoon mainland: new evaluation of origin, extension and dynamics, in: Barrocu, G. (Ed.), Proceedings 1st SWIM-SWICA Joint Saltwater Intrusion Conference, Cagliari-Chia Laguna, Italy - September 24-29 2006, pp. 195-204.

Donnici, S., Serandrei-Barbero, R., Canali, G., 2012. Evidence of climatic changes in the Venetian Coastal Plain (Northern Italy) during the last 40,000 years. Sediment. Geol. 281, 139-150.

Faegri, K., Iversen, I., 1989. Textbook of Pollen Analysis, fourth ed. Wiley, London.

Gambolati, G., Giunta, G., Putti, M., Teatini, P., Tomasi, L., Betti, I., Morelli, M., Berlamont, J., De Backer, K., Decouttere, C., Monbaliu, J., Yu, C. S., Broker, I., Christensen, E. D., Elfrink, B., Dante, A., Gonella, M., 1998. Coastal evolution of the Upper Adriatic Sea due to sea level rise and natural and anthropic land subsidence, in: Gambolati, G. (Ed.), CENAS. Coastline evolution of the Upper Adriatic Sea due to sea level rise and natural and anthropogenic land subsidence, Water Science and Technology Library - WSTL 28, pp. 1-34.

Heaton, T. J., Köhler, P., Butzin, M., Bard, E., Reimer, R. W., Austin, W., Bronk Ramsey, C., Hughen, K. A., Kromer, B., Reimer, P. J., Adkins, J., Burke, A., Cook, M. S., Olsen, J., Skinner, L. C., 2020. Marine20-the marine radiocarbon age calibration curve (0-55,000 cal BP). Radiocarbon 62, 779-820.

Horton, B. P., Khan, N. S., Cahill, N., Lee, J. S. H., Shaw, T. A., Garner, A. J., Kemp, A. C., Engelhart, Z. E., Rahmstorf, S., 2020. Estimating global mean sea-level rise and its uncertainties by 2100 and 2300 from an expert survey. npj Clim. Atmos. Sci. 3, 18. https://doi.org/10.1038/s41612-020-0121-5

IPCC, 2019. IPCC Special report on the ocean and cryosphere in a changing climate, Pörtner, H. O., Roberts, D. C., Masson-Delmotte, V., Zhai, P., Tignor, M., Poloczanska, E., Mintenbeck, K., Alegría, A., Nicolai, M., Okem, A., Petzold, J., Rama, B., Weyer, N. M. (eds.), Cambridge University Press.

Ivajnšič, D., Kaligarič, M., Fantinato, E., Del Vecchio, S., Buffa, G., 2018. The fate of coastal habitats in the Venice Lagoon from the sea level rise perspective. Appl. Geogr. 98, 34-42.

Kaniewski, D., Marriner, N., Morhange, C., Rius, D., Carre, M. B., Faivre, S., Van Campo, E., 2018. Croatia's Mid-Late Holocene (5200-3200 BP) coastal vegetation shaped by human societies. Quat. Sci. Rev. 200, 334-350.

Kaniewski, D., Marriner, N., Cheddadi, R., Vacchi, M., Rovere, A., Faivre, S., Otto, T., Luce, F., Carre, M. B., Benčić, G., Van Campo, E., 2021. Coastal submersions in the north-eastern Adriatic during the last 5200 years. Glob. Planet. Change 204, 103570. https://doi.org/10.1016/j.gloplacha.2021.103570

Khan, N. S., Horton, B. P., Engelhart, S., Rovere, A., Vacchi, M., Ashe, E. L., Törnqvist, T. E., Dutton, A., Hijma, M. P., Shennan, I., 2019. Inception of a global atlas of sea levels since the Last Glacial Maximum. Quat. Sci. Rev. 220, 359-371.

Kulp, S. A., Strauss, B. H., 2019. New elevation data triple estimates of global vulnerability to sea-level rise and coastal flooding. Nat. Commun. 10, 4844. https://doi.org/10.1038/s41467-019-12808-z

Lionello, P., Cavaleri, L., Nissen, K. M., Pino, C., Raicich, F., Ulbrich, U., 2012. Severe marine storms in the Northern Adriatic: characteristics and trends. Phys. Chem. Earth 40-41, 93-105.

Madricardo, F., Donnici, S., 2014. Mapping past and recent landscape modifications in the Lagoon of Venice through geophysical surveys and historical maps. Anthropocene 6, 86-96.

Magnan, A. K., Oppenheimer, M., Garschagen, M., Buchanan, M. K., Duvat, V. K. E., Forbes, D. L., Ford, J. D., Lambert, E., Petzold, J., Renaud, F. G., Sebesvari, Z., van de Wal, R. S. W., Hinkel, J., Pörtner, H. O., 2022. Sea level rise risks and societal adaptation benefits in low-lying coastal areas. Sci. Rep. 12, 10677. https://doi.org/10.1038/s41598-022-14303-w

Marriner, N., Kaniewski, D., Pourkerman, M., Vacchi, M., Melini, D., Seeliger, M., Morhange, C., Spada, G., 2023. Forecasted weakening of Atlantic overturning circulation could amplify

future relative sea-level rise in the Mediterranean: A review of climate and tide-gauge data links. Earth Sci. Rev. 242, 104456. https://doi.org/10.1016/j.earscirev.2023.104456

Mel, R., Lionello, P., 2014. Storm surge ensemble prediction for the city of Venice. WAF 29, 1044-1057.

Mel, R. A., Bendoni, M., Steffinlongo, D., 2022. Salt-marsh retreat on different time scales: issues and prospects from a 5-year monitoring campaign in the Venice Lagoon. Earth Surf. Process. Landforms 47, 1989-2005.

Milne, G. A., Long, A. J., Bassett, S. E., 2005. Modeling Holocene relative sea-level observations from the Caribbean and South America. Quat. Sci. Rev. 24, 1183-1202.

Milović M., Kovačić S., Jasprica N., Stamenković, V., 2016. Contribution to the study of Adriatic island flora: vascular plant species diversity in the Croatian island of Olib. Nat. Croat. 25, 25-54.

Miola, A., Bondesan, A., Corain, L., Favaretto, S., Mozzi, P., Piovan, S., Sostizzo, I., 2006. Wetlands in the Venetian Po Plain (northeastern Italy) during the Last Glacial Maximum: Interplay between vegetation, hydrology and sedimentary environment. Rev. Palaeobot. Palynol. 141, 53-81.

Miola, A., Favaretto, S., Sostizzo, I., Valentini, G., Asioli, A., 2010. Holocene salt marsh plant communities in the North Adriatic coastal plain (Italy) as reflected by pollen, non-pollen palynomorphs and plant macrofossil analyses. Veget. Hist. Archaeobot. 19, 513-529.

Nicholls, R. J., Cazenave, A., 2010. Sea-level rise and its impact on coastal zones. Science 328, 1517-1520.

Nicholls, R. J., Lincke, D., Hinkel, J., Brown, S., Vafeidis, A. T., Meyssignac, B., Hanson, S. E., Merkens, J., Fang, J., 2021. A global analysis of subsidence, relative sea-level change and coastal flood exposure. Nat. Clim. Chang. 11, 338-342.

Nosengo, N., 2003. Save our city! Nature 424, 608-609.

Oppenheimer, M., Glavovic, B. C., Hinkel, J., van de Wal, R., Magnan, A.K., Abd-Elgawad, A., Cai, R., Cifuentes-Jara, M., DeConto, R.M., Ghosh, T., Hay, J., Isla, F., Marzeion, B., Meyssignac, B., Sebesvari, Z., 2019. Sea level rise and implications for low-lying islands, coasts and communities, in: Pörtner, H. O., Roberts, D. C., Masson-Delmotte, V., Zhai, P., Tignor, M., Poloczanska, E., Mintenbeck, K., Alegría, A., Nicolai, M., Okem, A., Petzold,

J., Rama, B., Weyer, N. M. (Eds.), IPCC Special Report on the Ocean and Cryosphere in a Changing Climate, Cambridge University Press, pp. 321-445.

Piccoli, F., Merloni, N., 1989. Vegetation dynamics in coastal wetlands. An example in Northern Italy: the Bardello. Ecol. Mediterr. 15, 81-95.

Pirazzoli, P. A., 1987. Recent sea-level changes and related engineering problems in the lagoon of Venice (Italy). Prog. Oceanogr. 18, 323-346.

Pirazzoli, P. A., Tomasin, A., 2008. Sea-level and surges in the Adriatic Sea area: recent trends and possible near-future scenarios. Atti I.R. Ist. Veneto Sci. Lett. 166, 61-83.

Plater, A. J., Kirby, J. R., 2011. Sea-level change and coastal geomorphic response, in: Wolanksi, E., McLusky, D. (Eds), Treatise on estuarine and coastal science, Elsevier, London, Waltham, San Diego, pp. 39-72.

Reimer, P. J., Austin, W. E. N., Bard, E., Bayliss, A., Blackwell, P. G., Bronk Ramsey, C., Butzin, M., Cheng, H., Edwards, R. L., Friedrich, M., Grootes, P. M., Guilderson, T. P., Hajdas, I., Heaton, T. J., Hogg, A. G., Hughen, K. A., Kromer, B., Manning, S. W., Muscheler, R., Palmer, J. G., Pearson, C., van der Plicht, J., Reimer, R. W., Richards, D. A., Scott, E. M., Southon, J. R., Turney, C. S. M., Wacker, L., Adophi, F., Büntgen, U., Capano, M., Fahrni, S., Fogtmann-Schulz, A., Friedrich, R., Kudsk, S., Miyake, F., Olsen, J., Reinig, F., Sakamoto, M., Sookdeo, A., Talamo, S., 2020. The IntCal20 Northern Hemisphere radiocarbon calibration curve (0-55 cal kBP). Radiocarbon 62, 725-757.

Rizzetto, F., Tosi, L., 2011. Aptitude of modern salt marshes to counteract relative sea-level rise, Venice Lagoon (Italy). Geology 39, 755-758.

Roy, K., Peltier, W.R., 2018. Relative sea level in the Western Mediterranean basin: A regional test of the ICE-7G_NA (VM7) model and a constraint on Late Holocene Antarctic deglaciation. Quat. Sci. Rev. 183, 76-87.

Sarretta, A., Pillon, S., Molinaroli, E., Guerzoni, S., Fontolan, G., 2010. Sediment budget in the Lagoon of Venice, Italy. Cont. Shelf Res. 30, 934-949.

Schuerch, M., Spencer, T., Temmerman, S., Kirwan, M. L., Wolff, C., Lincke, D., McOwen, C. J., Pickering, M. D., Reef, R., Vafeidis, A. T., Hinkel, J., Nicholls, R. J., Brown, S., 2018. Future response of global coastal wetlands to sea-level rise. Nature 561, 231-234.

Serandrei-Barbero, R., Bertoldi, R., Canali, G., Donnici, S., Lezziero, A., 2005. Paleoclimatic record of the past 22,000 years in Venice (Northern Italy): Biostratigraphic evidence and chronology. Quat. Int. 140-141, 37-52.

Sfriso, A., Curiel, D., Rismondo, A., 2009. The lagoon of Venice, in: Cecere E., Petrocelli A., Izzo G., Sfriso A. (Eds.), Flora and Vegetation of the Italian Transitional Water Systems, CoRiLa-Multigraf-Spinea, pp. 17-80.

Shennan, I., Long, A. J., Horton, B. P., 2015. Handbook of Sea-Level Research. John Wiley & Sons, Chichester UK.

Shirzaei, M., Freymueller, J., Törnqvist, T.E., Galloway, D. L., Dura, T., Minderhoud, P. S. J., 2021. Measuring, modelling and projecting coastal land subsidence. Nat. Rev. Earth. Environ. 2, 40-58.

Silvestri, S., Marani, M., 2004. Salt-marsh vegetation and morphology: basic physiology, modelling and remote sensing observations, in: Fagherazzi, S., Blum, L., Marani, M. (Eds.), Ecogeomorphology of Tidal Marshes, American Geophysical Union, Coastal and Estuarine Monograph Series, pp. 5-25.

Spencer, T., Schuerch, M., Nicholls, R J., Hinkel, J., Lincke, D., Vafeidis, A. T., Reef, R., McFadden, L., Brown, S., 2016. Global coastal wetland change under sea-level rise and related stresses: The DIVA Wetland Change model. Glob. Planet. Change 139, 15-30.

Stancic; Z., Brigic, A., Liber, Z., Rusak, G., Franjic, J., Skvorc, Z., 2008. Adriatic coastal plant taxa and communities of Croatia and their threat status. Acta Bot. Gallica 155, 179-199.

Taramelli, A., Valentini, E., Piedelobo, L., Righini, M., Cappucci, S., 2021. Assessment of state transition dynamics of coastal wetlands in northern Venice lagoon, Italy. Sustainability 13, 4102. https://doi.org/10.3390/su13084102

Tay, C., Lindsey, E. O., Chin, S. T., McCaughey, J. W., Bekaert, D., Nguyen, M., Hua, H., Manipon, G., Karim, M., Horton, B. P., Li, T., Hille, E., 2022. Sea-level rise from land subsidence in major coastal cities. Nat. Sustain. 5, 1049-1057.

Tognin, D., D'Alpaos, A., Marani, M., Carniello, L., 2021. Marsh resilience to sea-level rise reduced by storm-surge barriers in the Venice Lagoon. Nat. Geosci. 14, 906-911.

Tommasini, L., Carniello, L., Ghinassi, M., Roner, M., D'Alpaos, A., 2019 Changes in the wind-wave field and related saltmarsh lateral erosion: inferences from the evolution of the Venice Lagoon in the last four centuries. Earth Surf. Process. Landforms 44, 1633-1646.

Tosi, L., Teatini, P., Strozzi, T., 2013. Natural versus anthropogenic subsidence of Venice. Sci. Rep. 3, 2710. https://doi.org/10.1038/srep02710

Tosi, L., Da Lio, C., Teatini, P., Strozzi, T., 2018. Land subsidence in coastal environments: knowledge advance in the Venice coastland by TerraSAR-X PSI. Remote Sens. 10, 1191. https://doi.org/10.3390/rs10081191

Troccoli, A., Zambon, F., Hodges, K. I., Marani, M., 2012. Storm surge frequency reduction in Venice under climate change. Clim. Change 113, 1065-1079.

Vacchi, M., Marriner, N., Morhange, C., Spada, G., Fontana, A., Rovere, A., 2016. Multiproxy assessment of Holocene relative sea-level changes in the western Mediterranean: sea level variability and improvements in the definition of the isostatic signal. Earth-Sci. Rev. 155, 172-197.

Vacchi, M., Joyse, K. M., Kopp, R. E., Marriner, N., Kaniewski, D., Rovere, A., 2021. Climate pacing of millennial sea-level change variability in the central and western Mediterranean. Nat. Commun. 12, 4013. https://doi.org/10.1038/s41467-021-24250-1

Williams, S. J., 2013. Sea-level rise implications for coastal regions. J. Coast. Res. 63, 184-196.

Wolff, W. J., 1968. The halophilous vegetation of the lagoons of Mesolonghi, Greece. Vegetatio 16, 95-134.

Woodroffe, C. D., Murray-Wallace, C. V., 2012. Sea-level rise and coastal change: the past as a guide to the future. Quat. Sci. Rev. 54, 4-11.

Wöppelmann, G., Zerbini, S., Marcos, M., 2006. Tide gauges and Geodesy: a secular synergy illustrated by three present-day case studies. C. R. Geoscience 338, 980-991.

Wu, P. C., Wei, M., D'Hondt, S., 2022. Subsidence in coastal cities throughout the world observed by InSAR. Geophys. Res. Lett. 49, e2022GL098477. https://doi.org/10.1029/2022GL098477

Zanchettin, D., Bruni, S., Raicich, F., Lionello, P., Adloff, F., Androsov, A., Antonioli, F., Artale, V., Carminati, E., Ferrarin, C., Fofonova, V., Nicholls, R. J., Rubinetti, S., Rubino,

A., Sannino, G., Spada, G., Thiéblemont, R., Tsimplis, M., Umgiesser, G., Vignudelli, S., Wöppelmann, G., Zerbini, S., 2021. Sea-Level Rise in Venice: Historic and Future Trends (Review Article). Nat. Hazards Earth Syst. Sci. 21, 2643-2678.
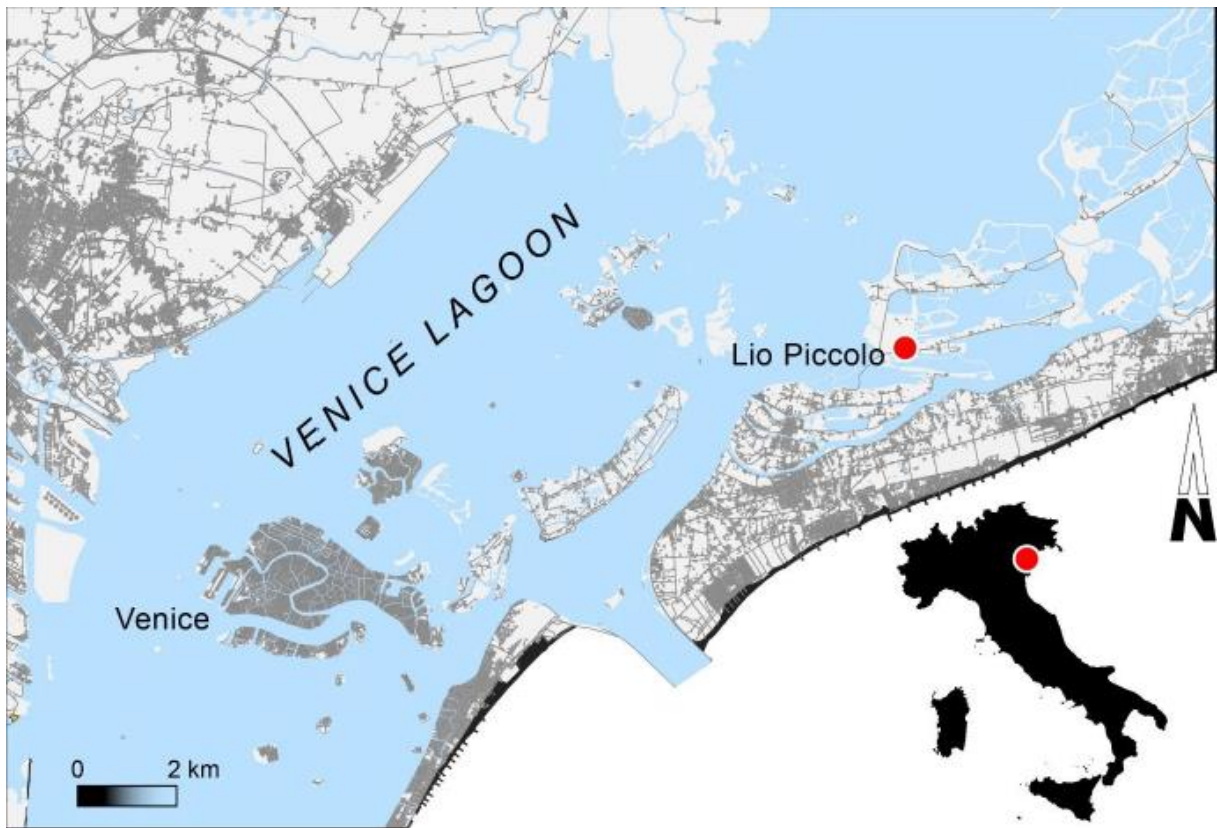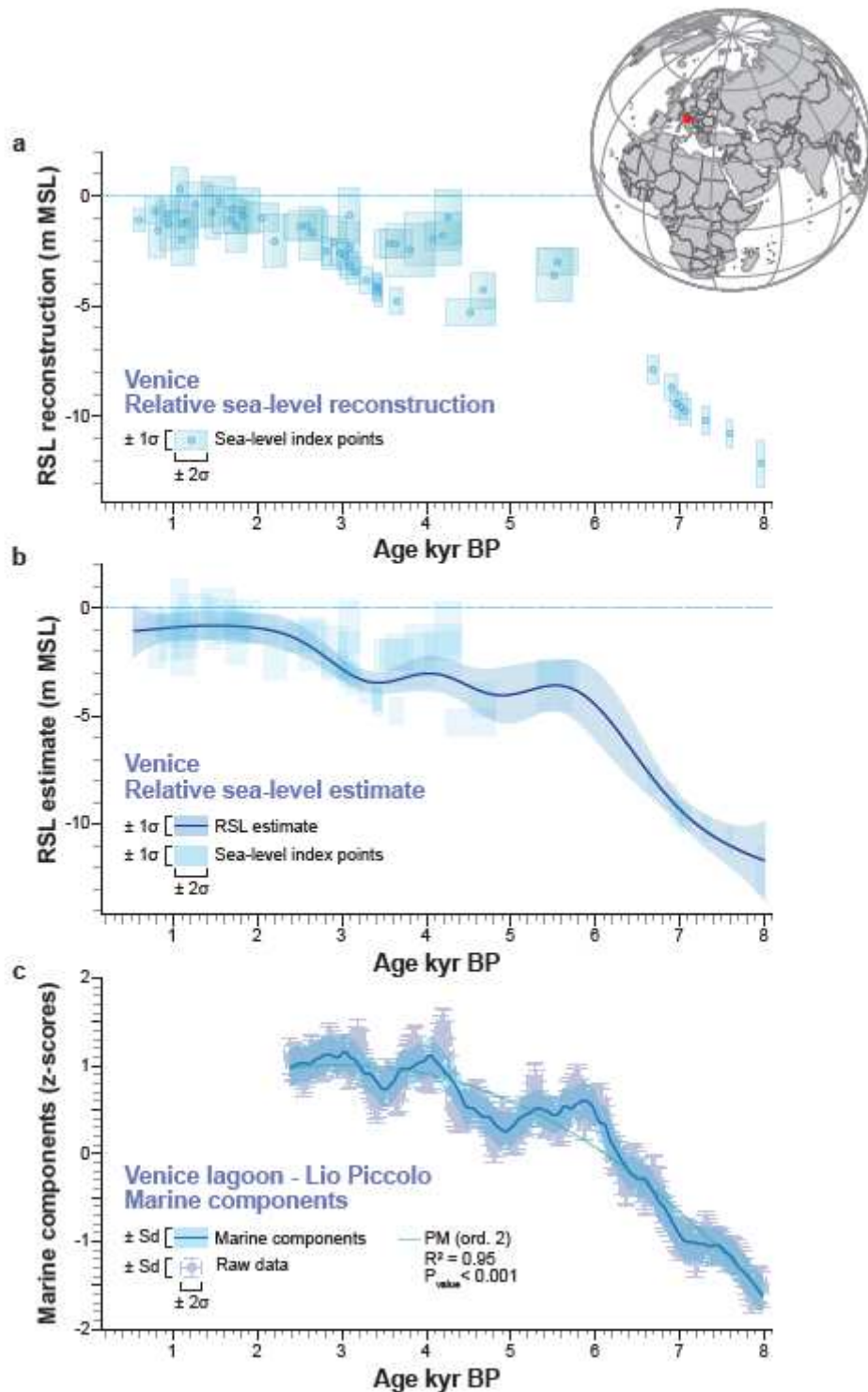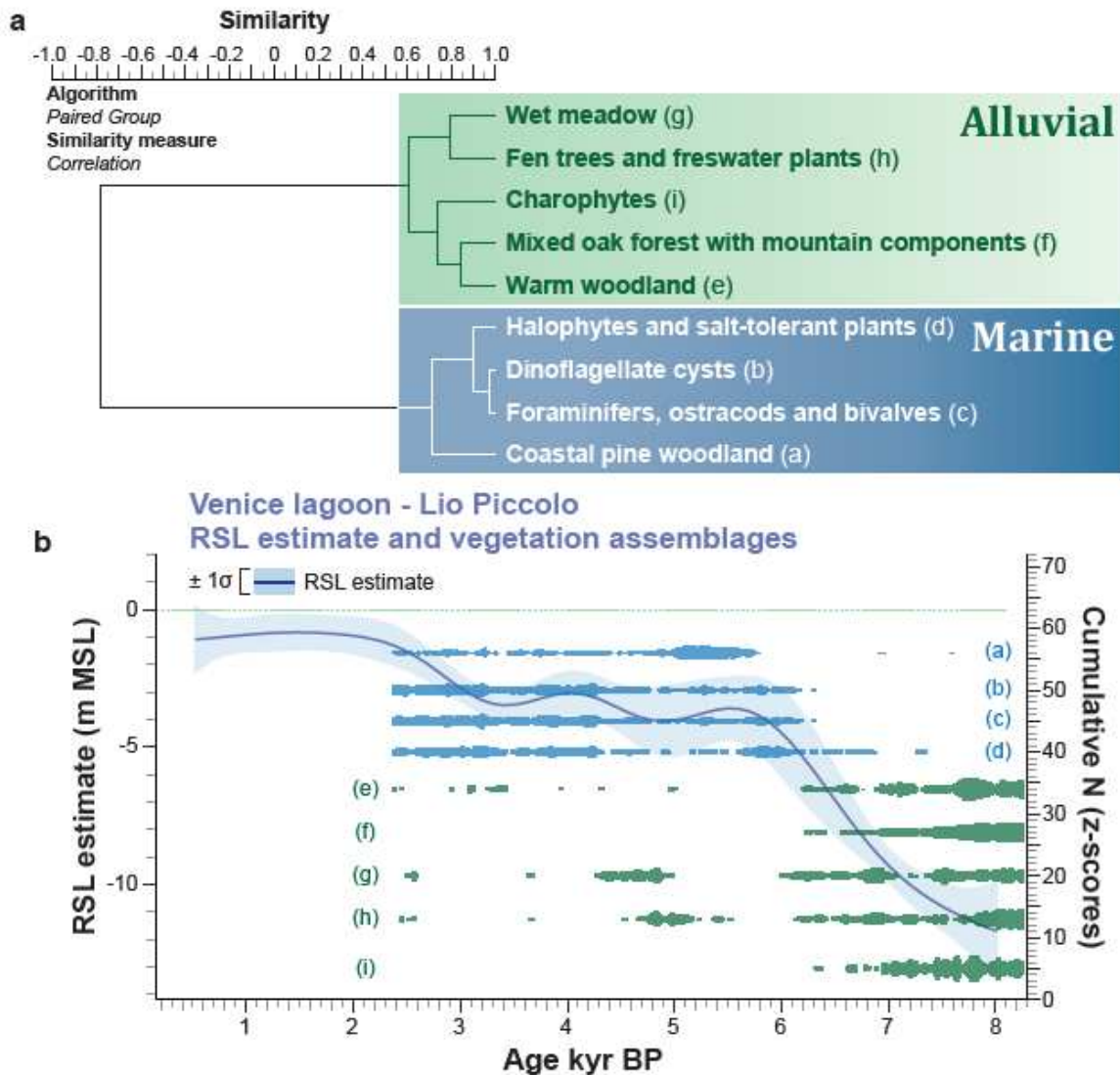
Figures

Figure 1. Geographical location of Lio Piccolo in the northern part of Venice Lagoon, Italy.

Figure 2. Standardized RSL reconstruction for Venice Lagoon - period 500-8000 BP. (**a**) The RSL history is based on 53 SLIPS. The blue boxes represent the SLIPS from the lagoons and salt marshes. The dimensions of the boxes denote the ± 1σ altitudinal and ± 2σ chronological errors associated with each SLIP. (**b**) Errors-In-Variables Integrated Gaussian Process model (EIV-IGP; Cahill et al., 2016) for RSL estimate (with the 1σ altitudinal error). (**c**) The marine

component signal (z-scores) display as a regular 20-yr chronological interpolation (termed raw data) and a 400-yr moving average (blue curve). The scores are plotted with the ± 2σ dating error and the standard deviation. The long-term trend was depicted as a polynomial model (green curve; termed PM; $P_{value} < 10^{-3}$).

Figure 3. Alluvial *versus* marine influence in Venice Lagoon. (**a**) Cluster analysis (algorithm *Paired group* - similarity measure *Correlation* - cophenetic correlation 0.99) showing the ordination of PdVs against charophytes and marine indicators. The green box emphasizes the alluvial influence while the blue box underlines the marine influence. (**b**) Spindle diagram (based on z-scores) contrasted with the RSL estimate (shown with the 1σ altitudinal error). The letter refers to each branch of the cluster analysis.
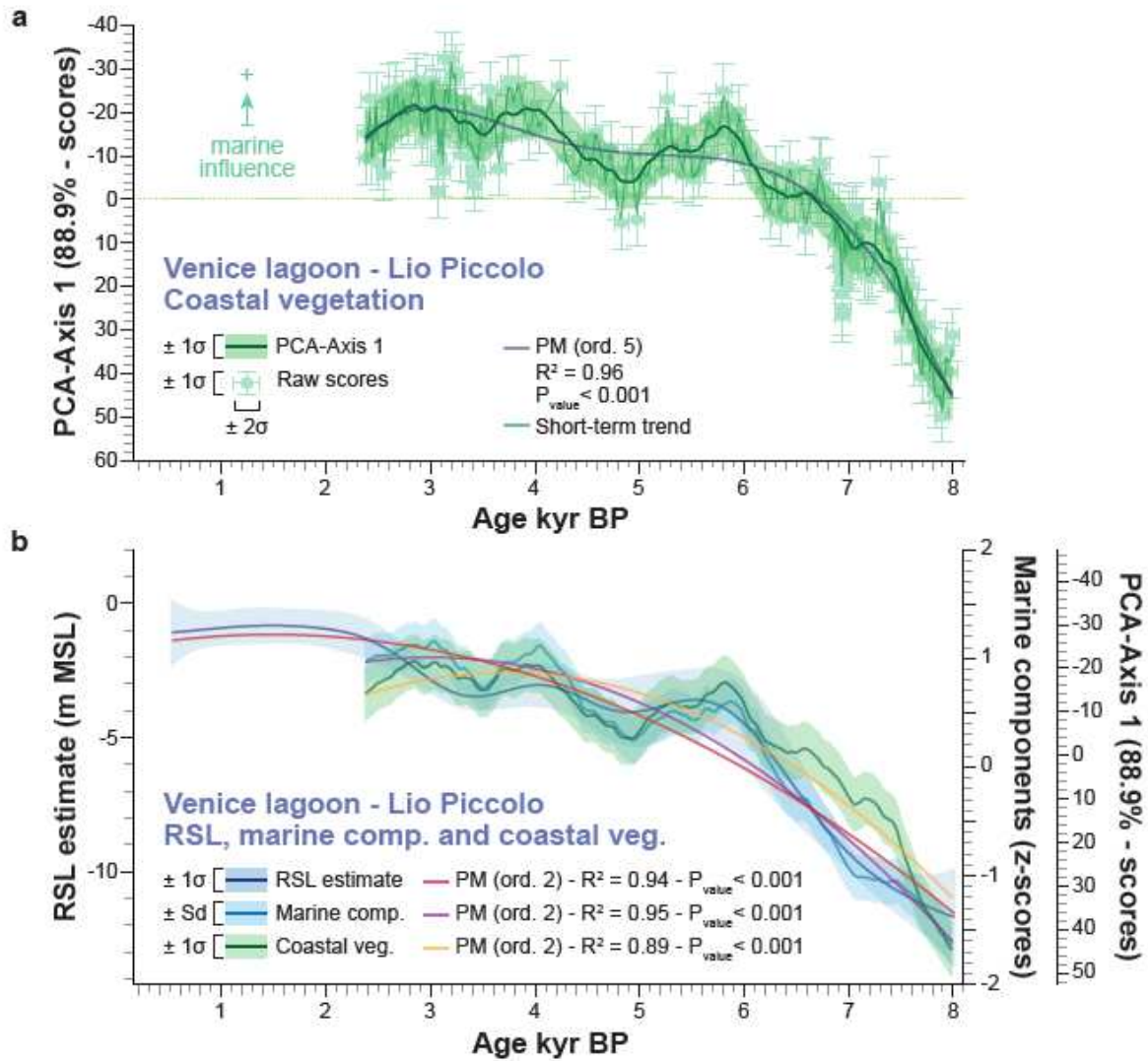
Figure 4. Ecosystem dynamic *versus* RSL estimate in Venice Lagoon. (**a**) PCA-axis 1 (coastal vegetation) shown as raw scores (with ± 1σ error and ± 2σ chronological calibration; termed short-term trend). The long-term trend is displayed as 400-yr moving average (green curve, with ± 1σ error) and polynomial model (termed PM; $P_{value} < 10^{-3}$). (**b**) The RSL estimate (dark blue curve, shown with the ± 1σ altitudinal error) is compared and contrasted with the coastal vegetation signal (green curve - PCA-Axis 1, 400-yr moving average, with ± 1σ error) and the marine components (light blue curve, 400-yr moving average, with the standard deviation). The long-term trends are displayed as polynomial models (termed PM; $P_{value} < 10^{-3}$).